circ-LRP6 contributes to osteosarcoma progression by regulating the miR-141-3p/HDAC4/HMGB1 axis

YALI YU[1], GUIXIANG DONG[1], ZIJUN LI[1], YAN ZHENG[1], ZHISONG SHI[2] and GUANGHUI WANG[2]

[1]Department of Laboratory, Zhengzhou Orthopedic Hospital, Zhengzhou, Henan 450052;
[2]Department of Orthopedic Surgery, Zhumadian Central Hospital, Zhumadian, Henan 463000, P.R. China

Received May 7, 2021; Accepted January 19, 2022

DOI: 10.3892/ijo.2022.5328

Abstract. Circular RNA-lipoprotein receptor 6 (circ-LRP6) serves a role in promoting the tumorigenesis of retinoblastoma, esophageal squamous cell cancer and oral squamous cell carcinoma; however, whether circ-LRP6 demonstrates the same effect in osteosarcoma (OS) is yet to be fully elucidated. The present study aimed to analyze the expression, role and potential molecular mechanism of circ-LRP6 in OS. The expression levels of circ-LRP6, microRNA (miR)-141-3p, histone deacetylase 4 (HDAC4) and high mobility group protein 1 (HMGB1) were evaluated by reverse transcription-quantitative PCR in OS tissues and cell lines. Cell Counting Kit-8, Transwell and Matrigel assays were conducted to evaluate cell proliferation, migration and invasion, respectively. Western blotting was also performed to determine HDAC4 and HMGB1 protein expression levels. Bioinformatics and dual-luciferase reporter assays were used to predict and analyze the interactions between circ-LRP6 and miR-141-3p, miR-141-3p and HDAC4, as well as between miR-141-3p and HMGB1. Additionally, RNA immunoprecipitation was performed to verify the association between circ-LRP6 and miR-141-3p. The results confirmed that circ-LRP6 was highly expressed in OS tissues and cell lines. In addition, circ-LRP6 negatively regulated the expression of miR-141-3p and, in turn, miR-141-3p negatively regulated HDAC4 and HMGB1 expression. Functional assays revealed that circ-LRP6 knockdown inhibited the proliferation, migration and invasion of OS cells, whereas the inhibition of miR-141-3p or the overexpression of either HDAC4 or HMGB1 partly reversed the inhibitory effect of circ-LRP6 knockdown. In summary, the present study determined that circ-LRP6 knockdown inhibited the proliferation, migration and invasion of OS cells by regulating the miR-141-3p/HDAC4/HMGB1 axis.

Correspondence to: Professor Guanghui Wang, Department of Orthopedic Surgery, Zhumadian Central Hospital, 747 Zhonghua Road West, Zhumadian, Henan 463000, P.R. China
E-mail: guanghuissrs@163.com

Key words: circular RNA-lipoprotein receptor 6, microRNA-141-3p, histone deacetylase 4, high mobility group protein 1, osteosarcoma

Introduction

Osteosarcoma (OS) is the most common primary bone tumor in children and adolescents; it is characterized by early metastasis and rapid progression (1). The treatment regimens of OS currently include neoadjuvant chemotherapy, surgical treatment and postoperative chemotherapy; however, the 5-year survival rate of patients remains at ~60% (2). The prognosis of patients with metastasis is considerably worse, with a 5-year survival rate of 20-30% (3). Therefore, there is an urgent requirement to identify novel therapeutic regimens or targets to improve the diagnosis and prognosis of patients with OS.

Circular (circ)RNAs are endogenous non-coding RNAs that are hundreds or thousands of bases in length and comprise a covalently closed structure (4). In recent years, an increasing number of studies have demonstrated that circRNAs are associated with a variety of human diseases, including cerebrovascular diseases, inflammatory diseases and neurological diseases (5-7). circRNAs are also closely associated with the occurrence of malignant tumors (8-11). Previous studies have revealed that circRNAs serve important roles in the progression of OS, directly regulating cell proliferation, apoptosis and metastasis (12,13). For instance, Ma *et al* (8) demonstrated that overexpression of circRNA ubiquitin associated protein 2 (circ-UBAP2) in OS cells promoted cell proliferation, invasion and migration by regulating microRNA (miRNA or miR)-204-3p/high-mobility group AT-hook 2 (HMGA2) signaling. In addition, Wen *et al* (11) reported that circRNA homeodomain-interacting protein kinase 3 (circ-HIPK3) promoted OS progression by modulating the miR-637/circ-HIPK3/histone deacetylase 4 (HDAC4) axis. Chen *et al* (12) also confirmed that circRNA calmodulin-regulated spectrin-associated protein 1 (circ-CAMSAP1) facilitated OS progression and metastasis by sponging miR-145-5p and subsequently regulating the expression of Friend leukemia integration 1. circRNA low-density lipoprotein receptor-related protein 6 (circ-LRP6), a newly discovered circRNA, has been detected in vascular smooth muscle cells, and has been determined to facilitate OS, oral squamous cell carcinoma and esophageal squamous cell cancer tumorigenesis (13-16). However, the role and mechanism of circ-LRP6 has not been fully elucidated in OS.

As a class of non-coding RNA, miRNAs are short endogenous RNAs that are 22-25 nucleotides in length (17,18). A large number of miRNAs have been reported to participate in OS progression, including miR-873, miR-9, miR-708-5p, miR-183 and miR-17-5p (19-23). miR-141-3p functions as a tumor suppressor in OS, colorectal cancer and gastric cancer (24-27). Additionally, in recent years, a number of studies have demonstrated that circRNAs can competitively bind to miRNAs, thereby eliminating the regulatory effect of miRNAs on their target genes and participating in tumor progression (28,29). For instance, in non-small cell lung carcinoma (NSCLC), circ_100395 inhibited NSCLC malignancy by sponging miR-141-3p and thereby increasing the expression levels of large tumor suppressor kinase 2 (30). Another study revealed that circRNA-100338 functions as a sponge of miR-141-3p, inhibiting the progression of hepatocellular carcinoma (31). Furthermore, circ-sine oculis-binding protein homolog, a novel circRNA, promoted cell migration by regulating the miR-141-3p/myosin phosphatase target subunit 1/phosphorylated myosin light chain 2 axis in prostate cancer (32). It has been reported that circ-LRP6 functions as an endogenous sponge for miR-145, miR-9-5p and miR-455 (14,33-34). However, it has not been reported whether circ-LRP6 sponges miR-141-3p, thus regulating the proliferation, invasion and migration of OS cells.

The HDAC4 gene is located in human chromatin 2q37.3 and is 8,980 base pairs in length, containing a total of 37 exons (35). Studies have determined that HDAC4 expression differs in various tissues and organs and serves an important role in the development and prognosis of tumors (35,36). In esophageal cancer, HDAC4 upregulation promotes tumor progression and is associated with poor survival (37). HDAC4 was also reported to promote OS cell proliferation and invasion (38). High mobility group box-1 (HMGB1) is highly expressed in a number of tumors, including lung, breast, head and neck, nasopharyngeal and colorectal cancer, indicating that it may be associated with the occurrence, invasion and metastasis of tumors (39-43).

miRNAs exert their biological functions by regulating the expression of their target genes at the transcriptional or post-transcriptional level (44). For example, it has been determined that HDAC4 is regulated by miR-200b-3p, miR-206, miR-29b and miR-873-3p (45-48). Furthermore, HMGB1 was demonstrated to be regulated by miR-451, miR-548b, miR-665, miR-142-3p and miR-129-5p (49-53). However, to the best of our knowledge, there are no studies that have assessed whether HDAC4 and HMGB1 are regulated by miR-141-3p and circ-LRP6 in OS.

The present study aimed to elucidate the expression, role and potential molecular mechanism of circ-LRP6 in OS and to explore the role of the circ-LRP6/miR-141-3p/HDAC4/HMGB1 axis in OS progression. The results of the current study may provide a potential target for the early diagnosis and clinical treatment of OS.

Materials and methods

Human tissue collection. OS and normal paracancerous tissues were obtained from 50 patients with OS (age range, 7-55 years; mean age, 21.52±10.15 years; 21 male and 29 female patients) who underwent radical resection at the Zhengzhou Orthopedic Hospital (Zhengzhou, China) between January 2018 and January 2019. Inclusion criteria for patient recruitment were as follows: i) Tissue obtained during surgery and diagnosed as OS by two pathologists; ii) the patient had not received adjuvant therapy, such as chemotherapy or radiotherapy, prior to surgery; and iii) the patient is willing to participate. The exclusion criteria were as follows: i) Patients with other diseases, including other tumors; ii) patients who received treatment prior to participation in the present study; and iii) patients who refused to participate in the study. The patients with OS were diagnosed by histopathology according to the tumor-node-metastasis (TNM) classification of the Union for International Cancer Control (UICC), and lung metastasis was determined according to CT imaging of lungs. All 50 patients with OS were studied in a follow-up. The median follow-up was 31 months (range, 3-60 months). All experiments were approved by the Ethics Committee of Zhengzhou Orthopedic Hospital (approval no. 201908) and samples were collected with the written informed consent of patients.

Cell culture. hFOB1.19 normal human osteoblast cells, along with OS cell lines (MG63, U-2OS, HOS and SaOS-2), were purchased from the American Type Culture Collection. hFOB1.19 cells were cultured in DMEM/F12 (Sangon Biotech Co., Ltd.) containing 10% FBS (HyClone; Cytiva) at 33.5˚C in 5% CO_2. All OS cell lines were cultured in DMEM (Sangon Biotech Co., Ltd.) containing 10% FBS at 37˚C in 5% CO_2.

Reverse transcription-quantitative PCR (RT-qPCR). Total RNA was extracted from tissue samples and cell lines using TRIzol® reagent (Invitrogen; Thermo Fisher Scientific, Inc.), after which the purified RNA was reverse transcribed into cDNA using the PrimeScript RT Reagent Kit (Takara Biotechnology Co., Ltd.) according to the manufacturer's protocol. The SYBR Green PCR Master Mix (Invitrogen; Thermo Fisher Scientific, Inc.) was used for qPCR using an ABI 7500 Real-Time PCR Instrument. β-actin was used as an internal control for circ-LRP6, HDAC4 and HMGB1, whereas U6 was used as an internal control for miR-141-3p. The relative expression level of each target gene was calculated using the $2^{-\Delta\Delta Cq}$ method (54). The thermocycling conditions were as follows: 95˚C for 15 sec; followed by 35 cycles at 60˚C for 60 sec, 72˚C for 40 sec. The expressions of circ-chaperonin-containing TCP1 subunit 2 (CCT2), circ-tripartite motif-containing 33 (TRIM33), circ-eukaryotic translation initiation factor 4 γ3 (EIF4G3) and circ-LRP6 in OS tissues and paracancerous tissues was also performed by RT-qPCR assay following the aforementioned experimental procedures. All the primer sequences used for qPCR are presented in Table I.

Construction of the pcDNA3.1-HMGB1 and HDAC4 overexpress plasmids. HOS and SaOS-2 cells in the logarithmic growth phase were trypsin digested and collected. HDAC4 and HMGB1 cDNA were subsequently cloned into pcDNA3.1 (pc; Invitrogen; Thermo Fisher Scientific, Inc.) to construct overexpression vectors. PCR was used to copy the HMGB1 (position of PCR amplified fragment on the chromosome, GRCh38:13:30462604-30461435) and HDAC4 (position of PCR amplified fragment on the chromosome,

Table I. Sequences of siRNAs, miR-141-3p inhibitor and mimic used for transfections, and primers used for reverse transcription-quantitative PCR.

Gene	Sequence (5' to 3')
si-circ-LRP6$^{\#1}$	AAGGATGTATTTATGTTATAATG
si-circ-LRP6$^{\#2}$	AACTAATGTATTTTTAGCTTAAG
si-NC	GCAGGGAGACTCGTCGCAATACC
miR-141-3p inhibitor	CCAUCUUUACCAGACAGUGUUA
Inhibitor NC	GCUGUCCCGGAGGAUCUUCACG
miR-141-3p mimic	UAACACUGUCUGGUAAAGAUGG
Mimic NC	CUCGACAAUCAGGUCACAGCGA
circ-LRP6 primer	F: CTTCTGTGCCTCTTGGTTA
	R: ACTTGATGATGCTCCTGTAA
miR-141-3p primer	F: CGGGCTAACACTGTCTGGTAAAG
	R: GTGCAGGGTCCGAGGTATTC
HDAC4	F: GTATGACACGCTGATGCT
	R: GCCACGGAGTTGAAGTAG
HMGB1	F: TCTTCCTCTTCTGCTCTGA
	R: ATCTTCCTCCTCTTCCTTCT
U6	F: CTCGCTTCGGCAGCACA
	R: AACGCTTCACGAATTTGCGT
β-actin	F: CCTGTACGCCAACACAGTGC
	R: ATACTCCTGCTTGCTGATCC
LRP6	F: TATTGTCCCCCGATGGGCTG
	R: AGTACATGAACCCACTTGAAGGA
circ-eukaryotic translation initiation factor 4 γ3	F: CCTACCCCATCCCCTTATTC
	R: ACCGTGCTGTAGACTGCTGAG
circ-chaperonin-containing TCP1 subunit 2	F: TCTTTGCATAGTCCCGGCAG
	R: AGAGAGGCATCTCGTCCACT
circ-tripartite motif-containing 33	F: GTATGCCGCCAAGAATGCAG
	R: CTTTGCCCAGAAGGTGGGAT

circ, circular RNA; F, forward; HDAC4, histone deacetylase 4; HMBG1, high mobility group protein 1; LRP6, lipoprotein receptor 6; miR, microRNA; NC, negative control; R, reverse; si, small interfering RNA.

GRCh38:13:239108176-239084216) DNA from the genome of both HOS and SaOS-2 cells using the following primers: HMGB1 forward, 5'-TCTTCCTCTTCTGCTCTGA-3' and reverse, 5'-ATCTTCCTCCTCTTCCTTCT-3'; and HDAC4 forward, 5'-GTATGACACGCTGATGCT-3' and reverse, 5'-GCCACGGAGTTGAAGTAG-3'. Thermocycling conditions were as follows: Initial denaturation at 95˚C for 5 min; followed by 34 cycles of denaturation at 95˚C for 30 sec, annealing at 62˚C for 30 sec, and extension at 72˚C for 60 sec; and a final extension at 72˚C for 7 min. PCR products were cleaned up by using the AxyGen® AxyPrep PCR Clean-Up Kit (Corning, Inc.) according to the manufacturer's protocol and linked to pGEM-T easy vector (Promega Corporation). *ApaI* and *NotI* enzyme were used to cut the pGEM-T and pcDNA3.1(-) vectors). T4 DNA ligase was used to ligate the pcDNA3.1(-) and the excised DNA fragments at 16˚C for 2 h using the T4 DNA Ligase kit (Takara Bio, Inc.) according to the manufacturer's protocol. Plasmids (GeneChem, Shanghai, China) were mixed in Opti-MEM (Gibco, Burlington, Canada) and incubated with the transfection reagent Lipofectamine® 3000 reagent (Invitrogen; Thermo Fisher Scientific, Inc.) for 20 min at room temperature. The resulting vectors (2 μg/μl) were transformed into *Escherichia coli* DH5α cells and cultured on LB plates containing 100 μg/ml ampicillin.

Cell grouping and transfections. The miR-141-3p mimic, mimic negative control (NC), miR-141-3p inhibitor, inhibitor NC, small interfering (si)RNA-circ-LRP6$^{\#1}$, si-circ-LRP6$^{\#2}$ and si-NC were designed and synthesized by Shanghai GenePharma Co., Ltd. HOS and SaOS-2 cells ($5x10^6$ cells/ml) were transfected as follows: i) The si-NC group transfected with 75 nM si-NC; ii) the si-circ-LRP6$^{\#1}$ group transfected with 75 nM si-circ-LRP6$^{\#1}$; iii) the si-circ-LRP6$^{\#2}$ group transfected with 75 nM si-circ-LRP6$^{\#2}$; iv) the si-circ-LRP6 + miR-141-3p inhibitor group transfected with 75 nM si-circ-LRP6$^{\#1}$ + 50 nM miR-141-3p inhibitor; v) the si-circ-LRP6$^{\#1}$ + pc-HDAC4 group transfected with 75 nM si-circ-LRP6$^{\#1}$ + 2 μg/μl pcDNA3.1-HDAC4; and vi) the si-circ-LRP6$^{\#1}$ + pc-HMGB1 group transfected with 75 nM si-circ-LRP6$^{\#1}$ + 1.8 μg/μl pcDNA3.1-HMGB1. All

cells were transfected using Lipofectamine® 3000 reagent (Invitrogen; Thermo Fisher Scientific, Inc.) at room temperature for 48 h and then used for subsequent experimentation. A total of 50 nM miR-141-3p mimic or mimic NC were transfected into HOS and SaOS-2 cells ($5x10^6$ cells/ml) using Lipofectamine 3000, as aforementioned, and used in subsequent experiments. The sequences of the transfected siRNAs, miRNA inhibitor, miRNA mimic and the respective controls are presented in Table I.

Cell Counting Kit (CCK)-8 assay. Transfected HOS and SaOS-2 cells were collected and the cell density was adjusted to $5x10^4$ cells/ml, after which 100 μl cell suspension was inoculated onto 96-well plates and cultured at 37˚C and 5% CO_2. After incubation for 1, 2, 3 and 4 days, 10 μl CCK-8 solution (Beyotime Institute of Biotechnology) was added and the cells were incubated at 37˚C for a further 4 h. The absorbance value at 450 nm was determined using a microplate reader.

Transwell assays. At 48 h after transfection, HOS and SaOS-2 cells were resuspended in serum-free RPMI-1640 medium (Gibco; Thermo Fisher Scientific, Inc.). To assess migration, 150 μl cell suspension was added into the upper chamber of a 24-well Transwell insert (pore size, 8 μM) at a density of $3x10^5$ cells/ml. To assess invasion, the upper chamber was pretreated with 50 μl Matrigel and air-dried at room temperature for 4 h, after which 150 μl cell suspension was added at a density of $3x10^5$ cells/ml. A total of 500 μl RPMI-1640 medium containing 10% FBS was added to the lower chamber and the cells were placed in an incubator at 37˚C and 5% CO_2 for 24 h. Subsequently, the cells in the lower chamber were washed twice with PBS, fixed with 4% paraformaldehyde for 30 min at room temperature and stained in 0.1% crystal violet for 15 min at room temperature. Five random fields of view of were observed, images were captured and cells were counted under a IX51 inverted light microscope (Olympus Corporation; magnification, x200).

Western blotting. Total protein was extracted from cells ($5x10^6$ cells/ml)using RIPA lysis buffer (Thermo Fisher Scientific, Inc.). After denaturing the protein samples at 100˚C for 10 min, their concentration was measured with a BCA protein assay kit (Pierce; Thermo Fisher Scientific, Inc.) according to the manufacturer's protocol. Protein (50 μg/lane) was then separated by 10% SDS-PAGE. The protein isolates were transferred onto PVDF membranes using the wet transfer method, after which the membranes were blocked with 1X TBS + 0.1% Tween-20 (TBST; Sangon Biotech Co., Ltd.) containing 10% skimmed milk powder for 2 h at room temperature. The membranes were washed with TBST for 3 times (10 minutes each time) and subsequently incubated with anti-HDAC4 (cat. no. ab235583; 1:1,000; Abcam), anti-HMGB1 (cat. no. ab79823; 1:10,000; Abcam) and anti-β-actin (cat. no. ab8227; 1:5,000; Abcam) primary antibodies at 4˚C overnight. HRP-conjugated secondary antibodies (cat. no. ab6721; 1:5,000; Abcam) were then added to membranes, which were then incubated for 2 h at room temperature. The membranes were washed with TBST for 3 times (10 minutes each time), and the protein bands were visualized using BeyoECL Plus ECL-like Western reagent (Beyotime Institute of Biotechnology) was used to visualize the bands. ImageJ version 1.8.0 (National Institutes of Health) was used for densitometric analysis; β-actin was used as an internal control.

RNA immunoprecipitation (RIP) assay. The binding of circ-LRP6 to argonaute RISC catalytic component 2 (AGO2) protein was detected using a Magna RIP RNA-Binding Protein Immunoprecipitation kit (MilliporeSigma). HOS and SaOS-2 cells ($8x10^6$ cells/ml) were collected and lysed according to the manufacturer's protocol, after which the cell extract was incubated for 10 min with antibodies against Argonaute2 (cat. no. ab32381; 1:2,000; Abcam) or immunoglobulin G (cat. no. ab109489; 1:5,000; Abcam) at room temperature. The magnetic bead antibody complex was resuspended in 900 μl RIP wash buffer. Cell extract (100 μl) was then added and incubated overnight at 4˚C. RNA was extracted from samples following digestion with protease K, after which the expression levels of circ-LRP6 and miR-141-3p were detected by RT-qPCR, aforementioned.

RNase R treatment. RNase R digestion was used to test the stability of RNA. RNA was isolated from HOS and SaOS-2 cells ($7x10^6$ cells/ml) using TRIzol® (Invitrogen; Thermo Fisher Scientific, Inc.), after which 10 μg RNA was digested with 40 U RNase R (Epicentre; Illumina, Inc.). Cells were divided into two groups: Mock control group and RNase R treatment group. The enrichment of circ-LRP6 and LRP6 mRNA was then determined by RT-qPCR, aforementioned.

Bioinformatics analysis. The Circular RNA Interactome (https://circinteractome.irp.nia.nih.gov/index.html) was used to predict the candidate downstream targets of circ-LRP6. TargetScan 7.2 (www.targetscan.org/vert_71) was conducted to predict the target genes of miR-141-3p. OS chip (GSE96964 dataset; https://www.ncbi.nlm.nih.gov/geo/geo2r/?acc=GSE96964) was used for analyzing the expression of circRNAs (circ-CCT2, circ-TRIM33 and circ-EIF4G3) (55).

Dual-luciferase reporter assay. Bioinformatics prediction analysis confirmed that miR-141-3p could bind with circ-LRP6, HDAC4 and HMGB1. The wild-type (Wt) 3'-untranslated regions (UTRs) of circ-LRP6, HDAC4 and HMGB1 were incorporated into pmirGLO plasmids (Promega Corporation). Complementary sequence mutation sites were designed and introduced into the 3'-UTRs circ-LRP6, HDAC4 and HMGB1, which were also constructed using the pMIR-reporter plasmid. The Wt or mutant (Mut) luciferase reporter plasmids were co-transfected with either miR-141-3p mimic (50 nM) or NC (50 nM) into HOS and SaOS-2 cells ($5x10^4$ cells/ml) using Lipofectamine® 3000 reagent (Invitrogen; Thermo Fisher Scientific, Inc.). At room temperature 48 h after transfection, luciferase activity was measured using the pmirGLO Dual-Luciferase Assay (Promega Corporation). Firefly luciferase activities were normalized to that of *Renilla* luciferase.

Statistical analysis. The data of the present study were statistically analyzed using SPSS 22.0 software (IBM Corp.). Data are expressed as the mean ± SD. Differences between OS and adjacent normal tissues were evaluated using a paired

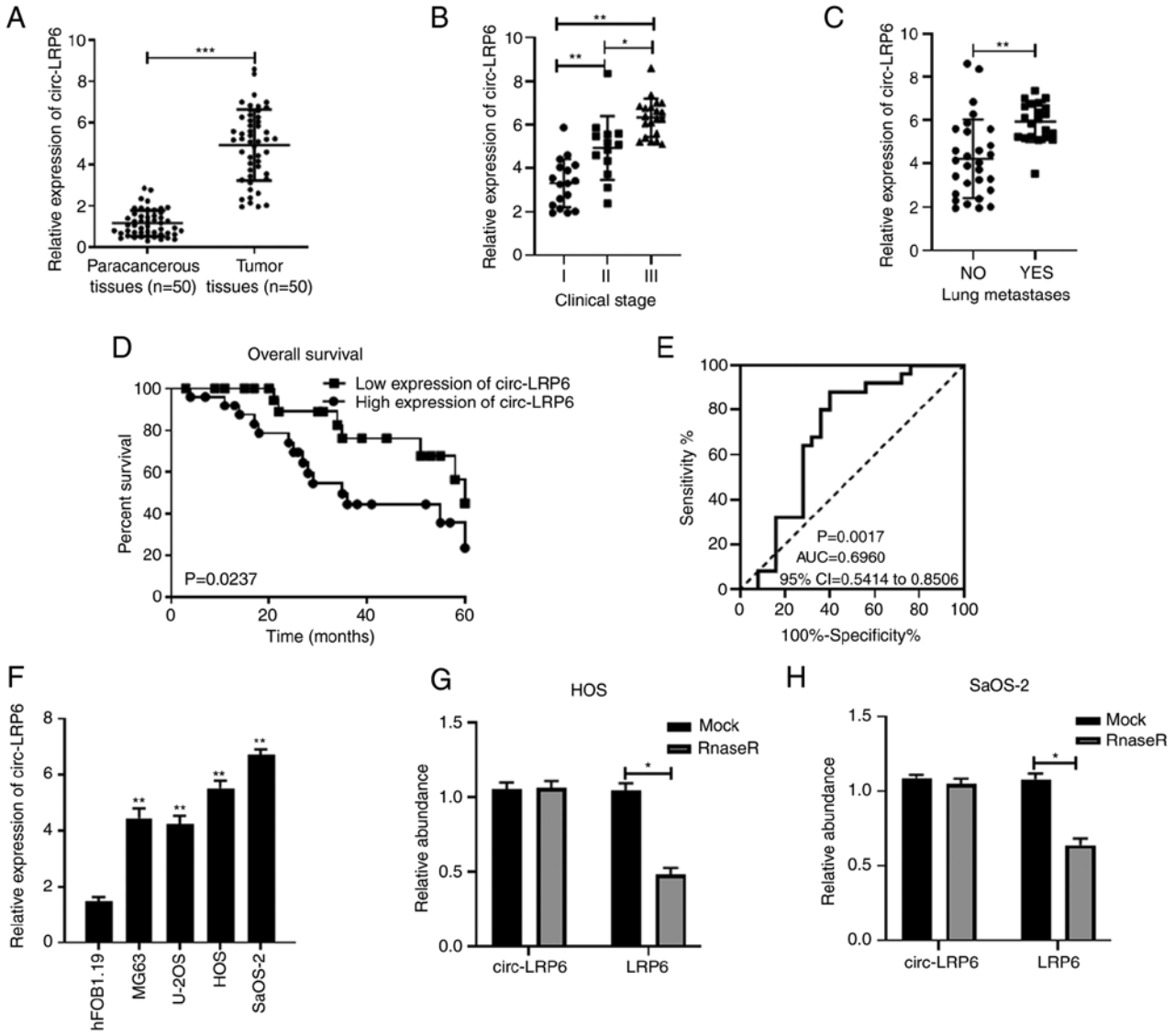

Figure 1. circ-LRP6 expression is upregulated in OS and associated with poor prognosis. (A) Expression levels of circ-LRP6 in 50 pairs of OS tissues and paracancerous tissues were analyzed by RT-qPCR. (B) circ-LRP6 expression levels in clinical stages I, II and III were analyzed by RT-qPCR. (C) circ-LRP6 expression levels in OS patients with and without lung metastasis were analyzed by RT-qPCR. (D) Comparison of overall survival in patients with high and low expression of circ-LRP6. (E) Receiver operating characteristic curve showing the diagnostic value of circ-LRP6 in distinguishing OS lung metastasis. (F) Expression levels of circ-LRP6 in OS cells and hFOB1.19 normal osteoblast cell line were analyzed by RT-qPCR. **P<0.01 vs. hFOB1.19. Detection of stability of circ-LRP6 in (G) HOS and (H) SaOS-2 cells by RNase R treatment. *P<0.05, **P<0.01, ***P<0.001. AUC, area under the curve; CI, confidence interval; circ, circular RNA; LRP6, lipoprotein receptor 6; OS, osteosarcoma; RT-qPCR, reverse transcription-quantitative PCR.

Student's t-test, whereas the differences between two groups of OS cells were evaluated using an unpaired Student's t-test. Differences between multiple groups of OS cells were evaluated using one-way ANOVA followed by a Tukey's post-hoc test. Kaplan-Meier analysis followed by log-rank tests were used to assess survival curves. Receiver operating characteristic (ROC) curve analysis was performed to assess the sensitivity and specificity of the measured markers. Fisher's exact test was used to investigate the relationship between clinicopathological features and circ-LRP6 expression, according to median expression levels. Correlations between circ-LRP6 and miR-141-3p, miR-141-3p and HDAC4, and miR-141-3p and HMGB1 were determined by performing Pearson's correlation analysis if the data are parametric and continuous. P<0.05 was considered to indicate a statistically significant difference.

Results

circ-LRP6 expression is upregulated in OS and is associated with poor prognosis. The OS chip dataset GSE96964 was analyzed and relevant literature was consulted; from these investigations several circRNAs (circ-CCT2, circ-TRIM33 and circ-EIF4G3 from GSE96964) and also circ-LRP6, from previous studies (14,55), were selected for RT-qPCR analysis in OS tissues (Fig. 1A and S1). It was found that circ-CCT2, circ-TRIM33, circ-EIF4G3 and circ-LRP6 was all overexpressed in OS tissues compared with expression in the paracancerous tissue (Fig. S1). As circ-LRP6 appeared to be more highly expressed compared with the other circRNAs, it was selected for further analysis. To investigate the relationship between circ-LRP6 expression and the clinicopathological features of patients, the 50 patients with OS were divided into

Table II. Association of circ-LRP6 expression with clinicopathological factors in osteosarcoma.

Clinicopathological feature	Total (n=50)	Expression level of circ-LRP6		P-value
		Low (n=25)	High (n=25)	
Sex				
Male	21	10	11	0.5
Female	29	15	14	
Age, years				
<20	26	14	12	0.389
≥20	24	11	13	
Tumor size, cm				
<8	23	13	10	0.285
≥8	27	12	15	
Tumor-node-metastasis stage				
I-II	30	19	11	0.021
III	20	6	14	
Distant metastasis				
Absent	29	20	9	0.002
Present	21	5	16	

circ-LRP6, circular RNA-lipoprotein receptor 6.

two groups according to the median expression of circ-LRP6: A high expression group (n=25) and a low expression group (n=25) (Table II). The association between circ-LRP6 expression levels and the clinical stage and lung metastases of patients was subsequently assessed. The results revealed that circ-LRP6 was significantly higher at clinical stage II and III compared with clinical stage I (Fig. 1B). Furthermore, an increased expression of circ-LRP6 was determined in patients exhibiting lung metastases compared with those that did not exhibit OS lung metastasis (Fig. 1C). circ-LRP6 expression was significantly associated with TNM stage and distant metastasis (Table II). Kaplan-Meier survival analysis demonstrated that the total survival rate of patients with high circ-LRP6 expression levels was significantly lower compared with that of patients with low circ-LRP6 expression levels (Fig. 1D). ROC curve analysis was used to evaluate the diagnostic value of circ-LRP6 expression levels in OS patients. The area under the curve value of circ-LRP6 was determined to be 0.6960 (95% confidence interval, 0.5414-0.8506; Fig. 1E).

The relative expression levels of circ-LRP6 in OS cell lines were also significantly higher compared with the hFOB1.19 normal osteoblast cell line (Fig. 1F). As the relative expression levels of circ-LRP6 were the highest in HOS and SaOS-2 cell lines, they were selected for subsequent experimentation. Additionally, to verify the stability of circ-LRP6, RNase treatment was applied, the results of which revealed that the expression of circ-LRP6 was not significantly altered when compared with the mock group, whereas the expression of LRP6 was significantly decreased, indicating the stability of circ-LRP6 (Fig. 1G and H).

circ-LRP6 knockdown inhibits the proliferation, migration and invasion of OS cells. The expression of circ-LRP6 in si-NC, si-circ-LRP6$^{1\#}$ and si-circ-LRP6$^{2\#}$ transfected OS cells was detected using RT-qPCR. The results revealed that the expression level of circ-LRP6 in the si-circ-LRP6$^{1\#}$ and si-circ-LRP6$^{2\#}$ groups was significantly lower compared with the NC group (Fig. 2A), which indicated that transfection had been a success and that transfected cells could be used for subsequent experiments. As si-circ-LRP6$^{\#1}$ had a better transfection efficiency, it was chosen for subsequent experiments. CCK-8, Transwell and Matrigel assays were performed to detect OS cell proliferation, migration and invasion, respectively. The results demonstrated that HOS and SaOS-2 cell proliferation in the si-circ-LRP6 groups was significantly inhibited compared with the respective si-NC group (Fig. 2B and C). In addition, compared with the si-NC group, the number of migratory and invasive cells in the si-circ-LRP6 group was significantly decreased (Fig. 2D and E, respectively). In conclusion, these data suggested that circ-LRP6 may serve as an oncogene in the progression of OS.

circ-LRP6 sponges miR-141-3p in OS. As circRNAs can competitively bind to miRNAs (12,13), the miRNAs that could bind to circ-LRP6 were predicted using the Circular RNA Interactome database. The top five miRNAs (miR-141-3p, miR-1208, miR-326, miR-330-5p and miR-513a-3p) that match circ-LRP6 along with their 'match degrees' (Fig. SII). miR-141-3p was selected for further analysis as the matched-degree between miR-141-3p and circ-LRP6 was relatively high compared with other matches, and due to the fact that miR-141-3p has been previously demonstrated to function as a tumor suppressor gene (24-27). Fig. 3A shows the pairing between miR-141-3p and circ-LRP6. miR-141-3p levels in the miR-141-3p mimic-transfected group were higher compared with the mimic NC group, indicating a

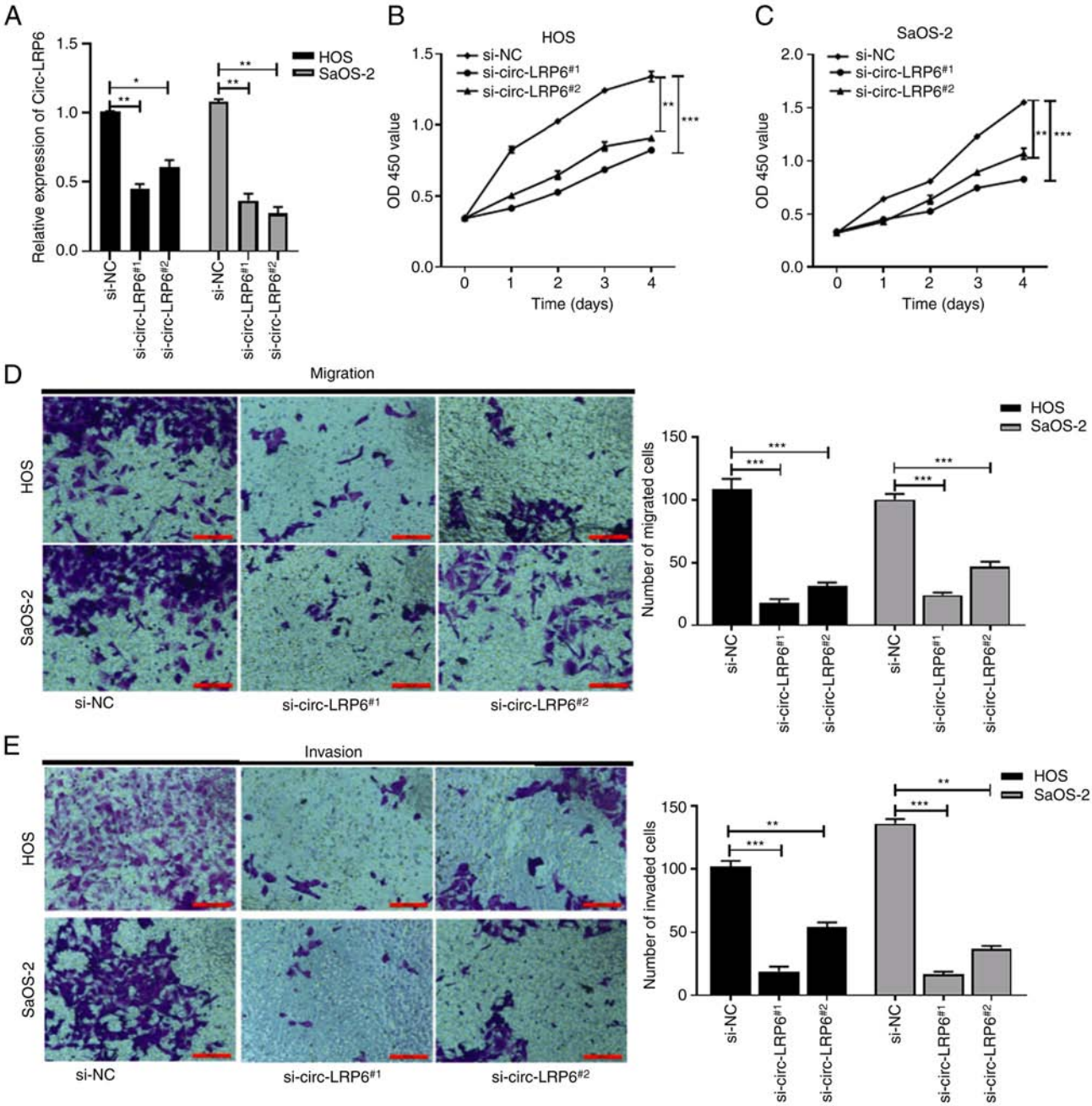

Figure 2. Knockdown of circ-LRP6 inhibits the proliferation, migration and invasion of OS cells. si-circ-LRP6$^{\#1}$, si-circ-LRP$^{\#2}$ or si-NC was transfected into HOS and SaOS-2 cells. (A) Expression levels of circ-LRP6 in the transfected OS cells were analyzed by reverse transcription-quantitative PCR. The proliferative ability of (B) HOS and (C) SaOS-2 cells was detected by CCK-8 assay. (D) Migratory and (E) invasive abilities of HOS and SaOS-2 cells was detected by Transwell and Matrigel assay, respectively. *P<0.05, **P<0.01, ***P<0.001. CCK-8, Cell Counting Kit-8; circ, circular RNA; LRP6, lipoprotein receptor 6; NC, negative control; OS, osteosarcoma; si, small interfering RNA.

successful transfection (Fig. 3B). The dual-luciferase assay results revealed that, compared with NC group, luciferase activity in the circ-LRP6-Wt + miR-141-3p group was significantly decreased, whereas no significant difference was identified between the luciferase activities of the circ-LRP6-Mut + miR-141-3p compared with the respective control group (Fig. 3C).

Results of the RIP experiments demonstrated that circ-LRP6 competitively bound to miR-141-3p in HOS and SaOS-2 cells (Fig. 3D and E). In addition, the results of RT-qPCR demonstrated that, compared with the si-NC group, the relative expression levels of miR-141-3p in the si-circ-LRP6 group was significantly increased (Fig. 3F), indicating that the expression of miR-141-3p may be regulated by circ-LRP6. RT-qPCR results further demonstrated that miR-141-3p expression was downregulated in OS tissues (Fig. 3G). miR-141-3p expression was determined to be negatively associated with circ-LRP6 expression (Fig. 3H). Kaplan-Meier survival curve analysis was subsequently demonstrated that the survival rate of patients with high miR-141-3p expression levels was significantly higher compared with patients with low miR-141-3p expression levels (Fig. 3I). The expression of miR-141-3p was also determined in OS cells. It was revealed that miR-141-3p was decreased in these cell lines (Fig. 3J).

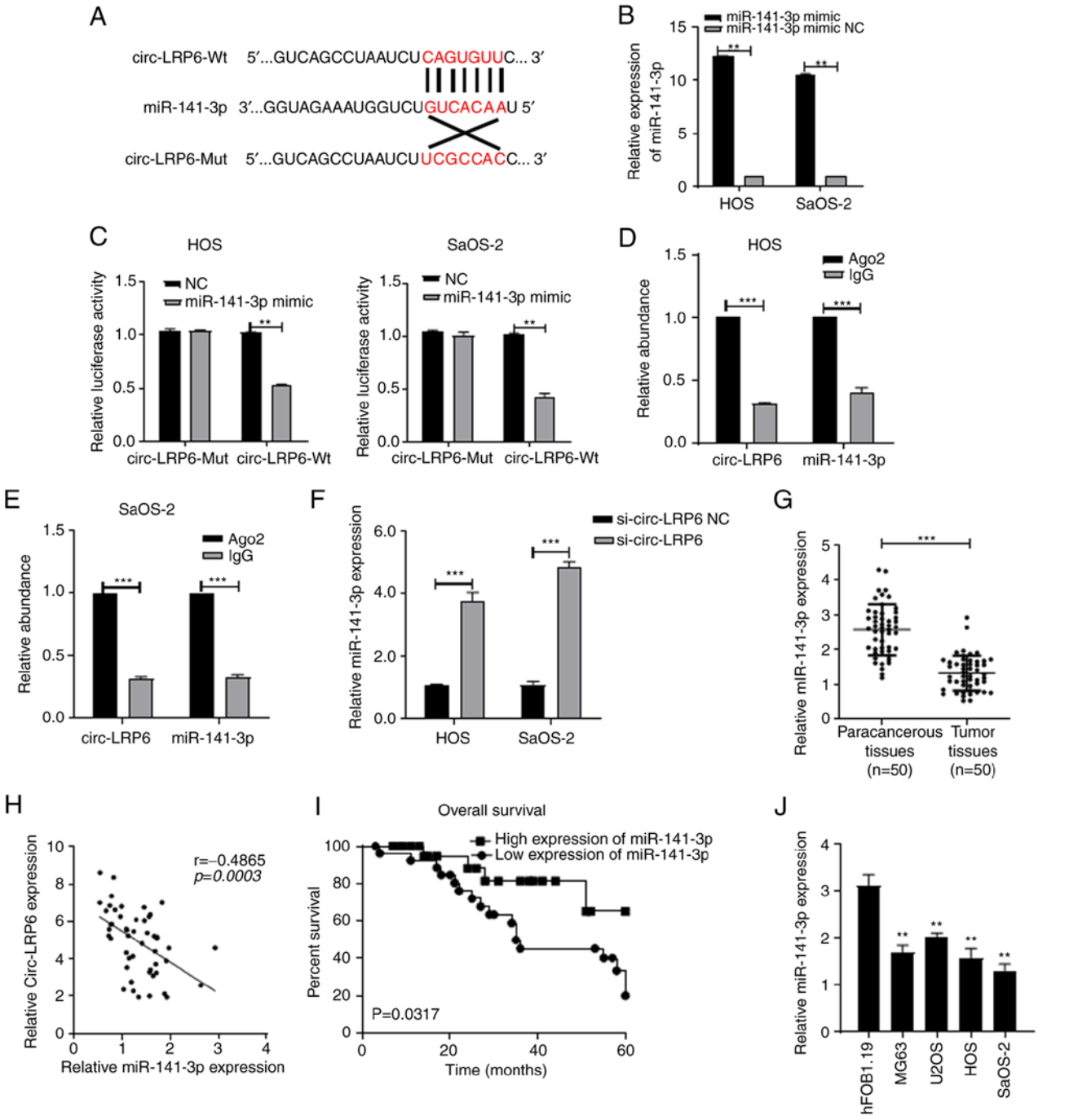

Figure 3. circ-LRP6 sponges miR-141 3p in OS. (A) Binding sites between circ-LRP6 and miR-141-3p. (B) Expression levels of miR-141-3p in HOS and SaOS-2 cells transfected with miR-141-3p inhibitor were analyzed by RT-qPCR. (C) The binding relationship between circ-LRP6 and miR-141-3p was verified by dual-luciferase assays in HOS and SaOS-2 cells. circ-LRP6 binding to miR-141-3p was verified by RIP assays in (D) HOS and (E) SaOS-2 cells. (F) Expression levels of miR-141-3p in HOS and SaOS-2 cells transfected with si-circ-LRP6 were analyzed by RT-qPCR. (G) Expression levels of miR-141-3p in 50 pairs of OS tissues and paracancerous tissues were analyzed by RT-qPCR. **P<0.05, ***P<0.001. (H) miR-141-3p expression is negatively correlated with circ-LRP6 expression in OS tissues. (I) Comparison of overall survival in patients with high and low expression levels of miR-141-3p. (J) Expression levels of miR-141-3p in OS cells and hFOB1.19 normal osteoblast cells were analyzed by RT-qPCR. **P<0.01 vs. hFOB1.19. Ago2, argonaute RISC catalytic component 2; circ, circular RNA; LRP6, lipoprotein receptor 6; miR, microRNA; Mut, mutant; NC, negative control; OS, osteosarcoma; RIP, RNA immunoprecipitation; RT-qPCR, reverse transcription-quantitative PCR; Wt, wild-type.

HDAC4 and HMGB1 are targets of miR-141-3p in OS. It has been reported that miRNAs can bind to the 3'-UTR of target genes and subsequently regulate the occurrence and progression of cancer (47-51). Therefore, the current study aimed to elucidate the targets of miR-141-3p. The TargetScan bioinformatics database predicted that miR-141-3p could bind to HDAC4 and HMGB1 (Fig. 4A and D). To verify these results, a dual-luciferase assay was performed, the data of which revealed that, when compared with the respective NC group, the luciferase activity of the HDAC4- or HMGB1-Wt + miR-141-3p mimic group was inhibited, whereas no significant difference was identified in the luciferase activities between HDAC4- or HMGB1-Mut+ miR-141-3p mimic group and the NC groups in the OS cell lines (Fig. 4B, C, E and F). RT-qPCR and western

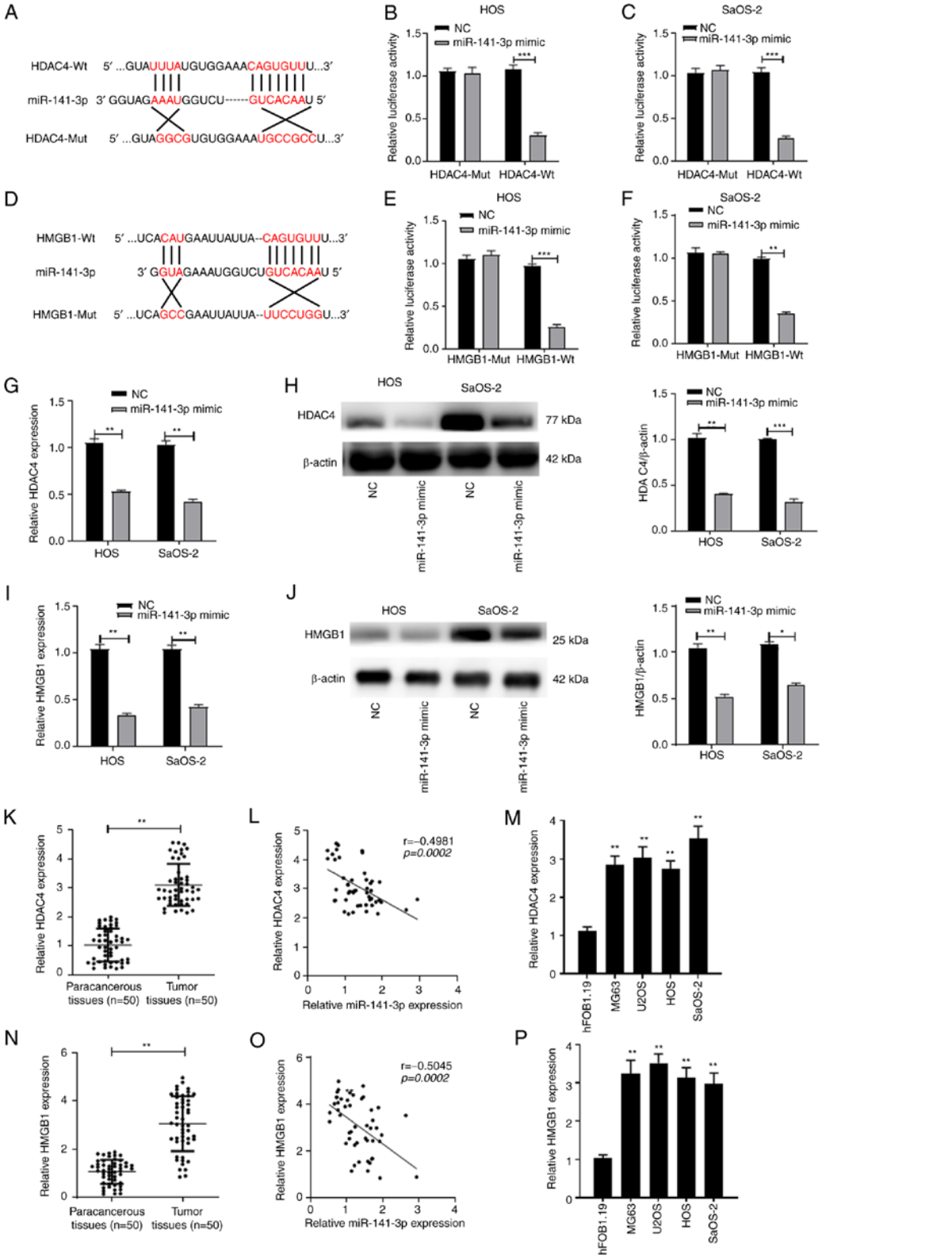

Figure 4. HDAC4 and HMGB1 are the targets of miR-141-3p in OS. (A) Binding sites between HDAC4 and miR-141-3p. Binding relationship between HDAC4 and miR-141-3p were verified by dual-luciferase assays (B) HOS and (C) SaOS-2 cells. (D) Binding sites between HMGB1 and miR-141-3p. Binding relationship between HMGB1 and miR-141-3p were verified by dual-luciferase assays in (E) HOS and (F) SaOS-2 cells. (G) mRNA and (H) protein expression levels of HDAC4 in HOS and SaOS-2 cells transfected with miR-141-3p mimic were analyzed by RT-qPCR and western blotting, respectively. (I) mRNA and (J) protein expression levels of HMGB1 in HOS and SaOS-2 cells transfected with miR-141-3p mimic were analyzed by RT-qPCR and western blotting, respectively. (K) Expression levels of HDAC4 mRNA in 50 pairs of OS tissues and paracancerous tissues were analyzed by RT-qPCR. *P<0.05, **P<0.01, ***P<0.001. (L) HDAC4 expression was negatively correlated with miR-141-3p expression in OS tissues. (M) Expression levels of HDAC4 mRNA in OS cells and in hFOB1.19 normal osteoblast cells were analyzed by RT-qPCR. **P<0.01 vs. hFOB1.19. (N) Expression levels of HMGB1 mRNA in 50 pairs of OS tissues and paracancerous tissues were analyzed by RT-qPCR. **P<0.01. (O) HMGB1 expression was negatively correlated with miR-141-3p expression in OS tissues. (P) Expression levels of HMGB1 mRNA in OS cell lines and in hFOB1.19 normal osteoblast cells were analyzed by RT-qPCR. **P<0.01 vs. hFOB1.19. HDAC4, histone deacetylase 4; HMBG1, high mobility group protein 1; miR, microRNA; Mut, mutant; NC, negative control; OS, osteosarcoma; RT-qPCR, reverse transcription-quantitative PCR; Wt, wild-type.

blotting data revealed that the mRNA and protein expression levels of HDAC4 and HMGB1 in the miR-141-3p mimic-transfected group was significantly decreased compared with the NC group (Fig. 4G-J). HDAC4 mRNA expression levels were then determined in OS tissues, and the results demonstrated that HDAC4 expression was upregulated compared with expression in the paracancerous tissue (Fig. 4K); this increased HDAC4 expression was negatively correlated with miR-141-3p expression in OS tissues (Fig. 4L). Similarly, HDAC4 was upregulated in OS cells compared with expression in hFOB1.19 cells (Fig. 4M). HMGB1 mRNA expression levels were also upregulated and negatively correlated with miR-141-3p expression in OS tissues (Fig. 4N and O); similarly, HMGB1 mRNA expression was upregulated in OS cells compared with hFOB1.19 (Fig. 4P).

circ-LRP6 promotes OS cell proliferation, migration and invasion by regulating the miR-141-3p/HDAC4 axis. The aforementioned results indicated that circ-LRP6 may promote OS cell malignancy, that circ-LRP6 sponged miR-141-3p and that HDAC4 was the target of miR-141-3p in OS. Therefore, to determine whether circ-LRP6 promoted OS progression by regulating the miR-141-3p/HDAC4 axis. OS cells transfected with either pcDNA3.1 empty vector or pc-HDAC4 overexpression vector; the results demonstrated that HDAC4 expression levels in the pc-HDAC4 group were significantly higher compared with the pcDNA3.1 group, indicating that transfection was successful (Fig. 5A). Additionally, miR-141-3p levels in the miR-141-3p inhibitor group were lower compared with the inhibitor NC group, indicating successful transfection (Fig. 5B). si-circ-LRP6, miR-141-3p inhibitor and pc-HDAC4 were co-transfected into HOS and SaOS-2 cells in various combinations, after which CCK-8 and Transwell assays were performed. The data revealed that inhibition of cell proliferation, migration and invasion induced by circ-LRP6 knockdown were partially reversed by miR-141-3p inhibition or HDAC4 overexpression (Fig. 5C-F). These data suggested that circ-LRP6 may facilitate OS progression through the miR-141-3p/HDAC4 axis.

circ-LRP6 promotes OS cell proliferation, migration and invasion by regulating the miR-141-3p/HMGB1 axis. As aforementioned, circ-LRP6 may promote OS cell malignancy and sponge miR-141-3p, and the results also revealed that HMGB1 was a target of miR-141-3p in OS. Therefore, whether circ-LRP6 promoted OS progression by regulating the miR-141-3p/HMGB1 axis was investigated. The expression of HMGB1 in OS cells transfected with pcDNA3.1 empty vector or pc-HMGB1 overexpression vector was detected using RT-qPCR, and the results demonstrated that HMGB1 expression levels in the pc-HMGB1 group were significantly higher compared with the pcDNA3.1 group, indicating that transfection had been successful (Fig. 6A). Subsequently, si-circ-LRP6, miR-141-3p inhibitor and pc-HMGB1 were variously co-transfected into HOS and SaOS-2 cells. Results from CCK-8, Transwell and Matrigel assays demonstrated that the significant inhibition of proliferation, migration and invasion of OS cells caused by circ-LRP6 knockdown were partially reversed by miR-141-3p inhibition or of HDAC4 overexpression (Fig. 6B-E). These results indicated that circ-LRP6 may facilitate OS progression through the miR-141-3p/HMGB1 axis.

Discussion

In recent years, non-coding RNAs, including circRNAs, long non-coding RNAs and miRNAs, have been widely reported as molecular markers for the genesis and development of various malignant tumors, including OS (8,23,56). For example, circ_0003074, circ-cytosolic 5' nucleotidase II and circ_0081001 can be used as biomarkers for the early diagnosis of OS (57-59). Additionally, various circRNAs mediate tumor progression by regulating cancer cell proliferation, invasion and migration. For example, Ma *et al* (8) revealed that circ-UBAP2 was highly expressed in OS tissues, and that high levels of circ-UBAP2 were positively associated with poor patient survival. Furthermore, Wang *et al* (60) demonstrated that circ-03955 overexpression could significantly promote the invasion, migration and epithelial to mesenchymal transformation of OS cells. Wan *et al* (61) also stated that circRNA-plasmacytoma variant translocation 1 facilitated OS cell invasion and metastasis. The results of the present study determined that circ-LRP6 was highly expressed in OS tissues and cell lines, and that low expression of circ-LRP6 significantly inhibited the proliferation, invasion and migration of OS cells. The GSE96964 OS microarray data identified several circRNAs (circ-CCT2, circ-TRIM33, circ-EIF4G3) and also circ-LRP6 were all highly-expressed in OS tissues (14,55). However, only circ-LRP6 was studied at present, and the roles of circ-CCT2, circ-TRIM33 and circ-EIF4G3 from GSE96964 shall be investigated in future studies.

circRNAs act as competing endogenous RNAs to sponge miRNAs, and to subsequently regulate the expression of target genes (28,56,61,62). As Ma *et al* (8) reported, circ-UBAP2 knockdown inhibited the progression of OS cells by upregulating the expression of miR-204-3p and, thus, downregulating the expression of its target gene, HMGA2. In addition, Wen *et al* (11) reported that circ_HIPK3 promoted OS cell proliferation, migration and invasion by regulating miR-637 and HDAC4 signaling. As a tumor suppressor-related miRNA, miR-141-3p has been reported to serve as a tumor suppressor in several types of cancer, including OS (24-27). With use of a Circular RNA Interactome database, the present study predicted that circ-LRP6 may have a binding site with miR-141-3p, which was confirmed by dual luciferase assay. Following circ-LRP6 knockout, OS cell proliferation, migration and invasion were inhibited, whereas combined miR-141-3p inhibition reversed this effect, which suggested that circ-LRP6 may facilitate the malignant behavior of OS cells by competitively binding to miR-141-3p.

Previous studies have demonstrated that miRNAs can bind to the 3'-UTRs of target genes to achieve post-transcriptional regulation, thereby modulating the occurrence and progression of related diseases (20-25,45,63). In the present study, TargetScan bioinformatics analysis and luciferase assays confirmed that miR-141-3p bound to the 3'-UTR of HDAC4 and HMGB1. HDAC4 belongs to the HDAC family and serves a role mainly through histone acetyltransferases (37). HDACs regulate the expression of a variety of genomic proteins to regulate cell apoptosis and participate in the

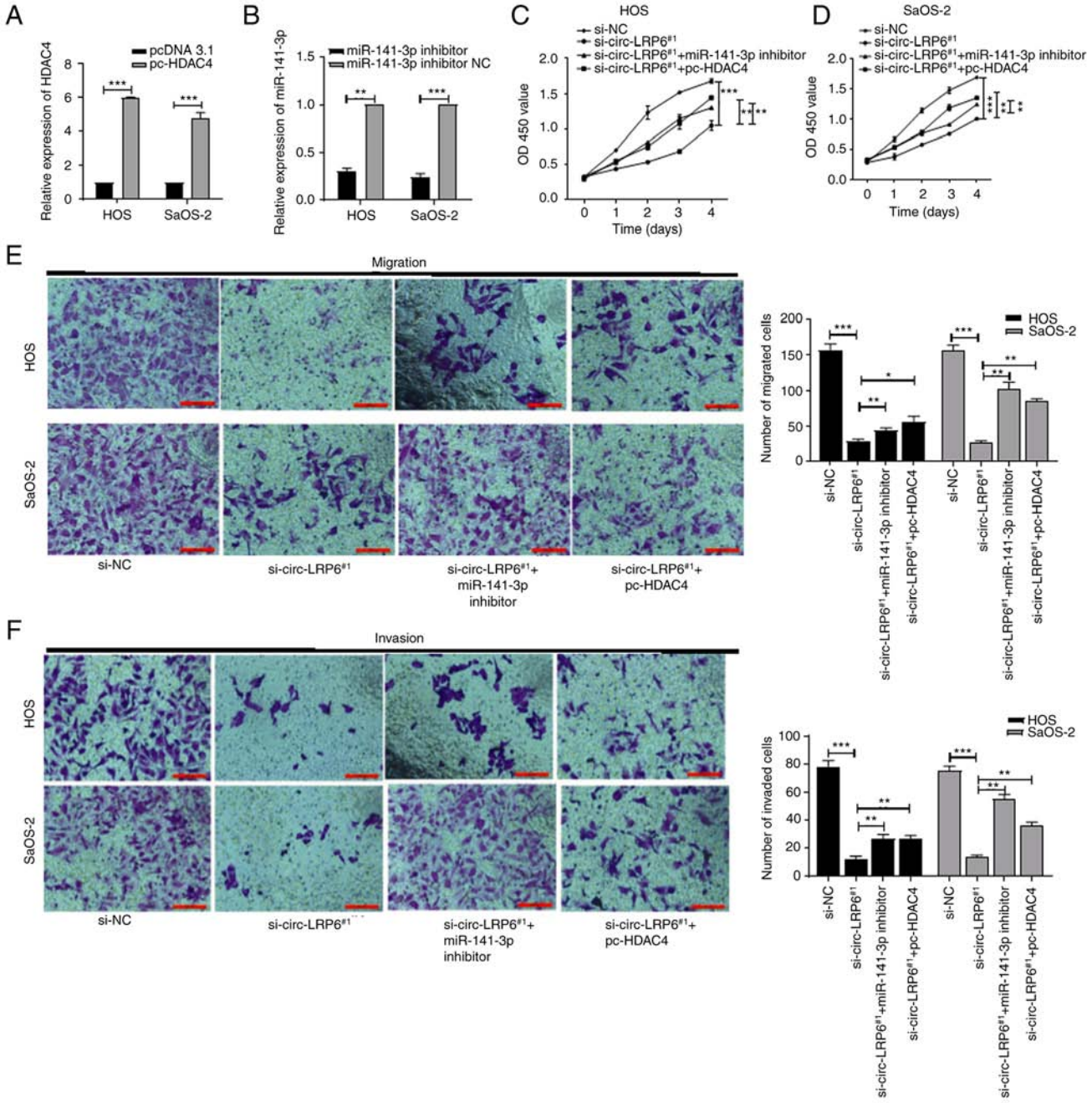

Figure 5. circ-LRP6 promotes OS cell proliferation, migration and invasion by regulating the miR-141-3p/HDAC4 axis. HOS and SaOS2 OS cells were co-transfected with various combination of si-circ-LRP6, miR-141-3p inhibitor and pc-HDAC4. (A) Expression levels of HDAC4 mRNA in HOS and SaOS-2 cells transfected with pc-HDAC4 were analyzed by RT-qPCR. (B) Expression levels of miR-141-3p in HOS and SaOS-2 cells transfected with miR-141-3p mimic were analyzed by RT-qPCR. The proliferative ability of (C) HOS and (D) SaOS-2 cells was detected by CCK-8 assay. (E) The migratory ability of HOS and SaOS-2 cells was detected by Transwell assay. (F) The invasive ability of HOS and SaOS-2 cells was detected by Matrigel assay. *P<0.05, **P<0.01, ***P<0.001. CCK-8, Cell Counting Kit-8; circ, circular RNA; HDAC4, histone deacetylase 4; LRP6, lipoprotein receptor 6; miR, microRNA; NC, negative control; OS, osteosarcoma; RT-qPCR, reverse transcription-quantitative PCR; si, small interfering RNA.

occurrence and development of tumors (38-41). Previous studies have revealed that HDAC4 is abnormally expressed in a variety of tumors, including glioma, breast cancer, ovarian cancer and OS (35,38,64,65). HMGB1 is a type of chromatin nucleoprotein that is associated with tumor invasion and metastasis (66-68). It is highly expressed in a number of malignant tumors, including cervical cancer, breast cancer and endometrial carcinoma (40,52,67). It is also associated with pathological stage, degree of invasion and degree of tumor metastasis (68). The present study showed that HDAC4 and HMGB1 were highly expressed in OS tissues and cells, which is consistent with previous studies (11,65). Furthermore, the protein expression levels of HDAC4 and HMGB1 were significantly decreased after miR-141-3p overexpression, suggesting that miR-141-3p may bind to HDAC4 and HMGB1 to downregulate their expression.

A number of studies have demonstrated that circRNAs act as competitive RNAs to adsorb various miRNAs, thus affecting the expression of target mRNAs (10-15). As aforementioned, circ-LRP6 promoted OS cell malignancy by downregulating miR-141-3p. Furthermore, as

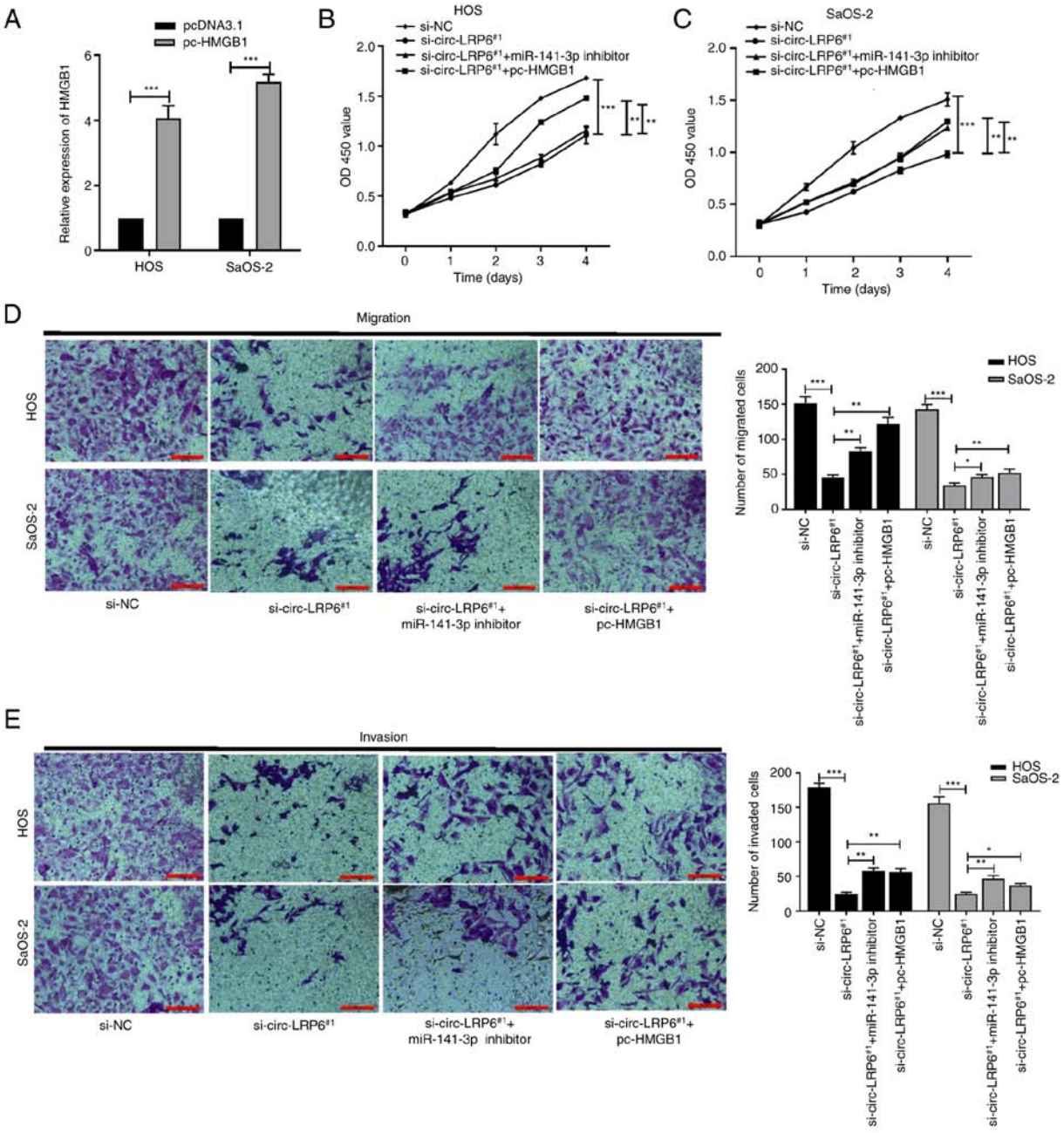

Figure 6. circ-LRP6 promotes OS cell proliferation, migration and invasion by regulating the miR-141-3p/HMGB1 axis. si-circ-LRP6, miR-141-3p inhibitor and pc-HMGB1 were variously co-transfected into OS cells. (A) Expression levels of HMGB1 mRNA in HOS and SaOS-2 cells transfected with pc-HMGB1 were analyzed by reverse transcription-quantitative PCR. The proliferative ability of (B) HOS and (C) SaOS-2 cells was detected by CCK-8 assay. (D) The migratory ability of HOS and SaOS-2 cells was detected by Transwell assay. (E) The invasive ability of HOS and SaOS-2 cells was detected by Matrigel assay. *P<0.05, **P<0.01, ***P<0.001. CCK-8, Cell Counting Kit-8; circ, circular RNA; HMBG1, high mobility group protein 1; LRP6, lipoprotein receptor 6; miR, microRNA; NC, negative control; OS, osteosarcoma; si, small interfering RNA.

miR-141-3p could bind to HDAC4 and HMGB1, it was hypothesized that circ-LRP6 promoted OS cell malignancy by regulating the miR-141-3p/HDAC4/HMGB1 axis. A series of functional assays revealed that circ-LRP6 silencing inhibited cell proliferation, migration and invasion, while miR-141-3p inhibition or HDAC4 and HMGB1 overexpression could reverse these effects, suggesting that the circ-LRP6/miR-141-3p/HDAC4/HMGB1 axis participated in OS progression. However, there are certain limitations to the present study. For example, *in vivo* experiments were not performed to elucidate the effects of circ-LRP6 on OS tumorigenesis and lung metastasis.

In conclusion, the present results revealed that circ-LRP6 was upregulated in OS tissues and cells, and that circ-LRP6 could downregulate the expression of miR-141-3p and upregulate HDAC4 and HMGB1 expression, thereby promoting the proliferation, migration and invasion of OS cells. To the best of our knowledge, the current study was the first to demonstrate that the circ-LRP6/miR-141-3p/HDAC4/HMGB1 axis participated in OS progression, which provides a new area of research for the exploration of OS pathogenesis. However, as there have been no animal experiments to confirm the regulatory mechanism of circ-LRP6 *in vivo*, further experimentation is required. Additionally, future studies should assess whether

circ-LRP6 is suitable for the clinical treatment of patients with OS.

Acknowledgements

Not applicable.

Funding

The present study was supported by Medical Science and Technology Project of Henan Province in 2020 (LHGJ20200759).

Availability of data and materials

The datasets used during the present study are available from the corresponding author upon reasonable request.

Authors' contributions

YY designed the study, performed the experiments and drafted the manuscript. GD and ZL analyzed the data. YZ and ZS analyzed the data for the work and revised the manuscript. GW contributed to the conception or design of the work, analyzed the data for the work and managed the project administration. YY and GW confirmed the authenticity of all the raw data. All authors read and approved the final manuscript.

Ethics approval and consent to participate

The present study was approved (approval no. 201908) by the Ethics Committee of Zhengzhou Orthopedic Hospital (Zhengzhou, China). Written informed consent was obtained from all patients.

Patient consent for publication

Not applicable.

Competing interests

The authors declare that they have no competing interests.

References

1. Sangle NA and Layfield LJ: Telangiectatic osteosarcoma. Arch Pathol Lab Med 136: 572-576, 2012.
2. Strobel O, Neoptolemos J, Jäger D and Büchler MW: Optimizing the outcomes of pancreatic cancer surgery. Nat Rev Clin Oncol 16: 11-26, 2019.
3. Harrison DJ, Geller DS, Gill JD, Lewis VO and Gorlick R: Current and future therapeutic approaches for osteosarcoma. Expert Rev Anticancer Ther 18: 39-50, 2018.
4. Li Z, Ruan Y, Zhang H, Shen Y, Li T and Xiao B: Tumor-suppressive circular RNAs: Mechanisms underlying their suppression of tumor occurrence and use as therapeutic targets. Cancer Sci 110: 3630-3638, 2019.
5. Zhang F, Zhang R, Zhang X, Wu Y, Li X, Zhang S, Hou W, Ding Y, Tian J, Sun L and Kong X: Comprehensive analysis of circRNA expression pattern and circRNA-miRNA-mRNA network in the pathogenesis of atherosclerosis in rabbits. Aging (Albany NY) 10: 2266-2283, 2018.
6. Xu Y, Xu X, Ocansey DKW, Cao H, Qiu W, Tu Q and Mao F: CircRNAs as promising biomarkers of inflammatory bowel disease and its associated-colorectal cancer. Am J Transl Res 13: 1580-1593, 2021.
7. Wu F, Han B, Wu S, Yang L, Leng S, Li M, Liao J, Wang G, Ye Q, Zhang Y, *et al*: Circular RNA TLK1 aggravates neuronal injury and neurological deficits after ischemic stroke via miR-335-3p/TIPARP. J Neurosci 39: 7369-7393, 2019.
8. Ma W, Xue N, Zhang J, Wang D, Yao X, Lin L and Xu Q: circUBAP2 regulates osteosarcoma progression via the miR-204-3p/HMGA2 axis. Int J Oncol 58: 298-311, 2021.
9. Liu S, Zhang J, Zheng T, Mou X and Xin W: Circ_WWC3 overexpression decelerates the progression of osteosarcoma by regulating miR-421/PDE7B axis. Open Life Sci 16: 229-241, 2021.
10. Huo S and Dou D: Circ_0056285 regulates proliferation, apoptosis and glycolysis of osteosarcoma cells via miR-1244/TRIM44 axis. Cancer Manag Res 13: 1257-1270, 20210.
11. Wen Y, Li B, He M, Teng S, Sun Y and Wang G: circHIPK3 promotes proliferation and migration and invasion via regulation of miR-637/HDAC4 signaling in osteosarcoma cells. Oncol Rep 45: 169-179, 2021.
12. Chen Z, Xu W, Zhang D, Chu J, Shen S, Ma Y, Wang Q, Liu G, Yao T, Huang Y, *et al*: circCAMSAP1 promotes osteosarcoma progression and metastasis by sponging miR-145-5p and regulating FLI1 expression. Mol Ther Nucleic Acids 23: 1120-1135, 2020.
13. Hall IF, Climent M, Quintavalle M, Farina FM, Schorn T, Zani S, Carullo P, Kunderfranco P, Civilini E, Condorelli G and Elia L: Circ_Lrp6, a circular RNA enriched in vascular smooth muscle cells, acts as a sponge regulating miRNA-145 function. Circ Res 124: 498-510, 2019.
14. Zheng S, Qian Z, Jiang F, Ge D, Tang J, Chen H, Yang J, Yao Y, Yan J, Zhao L, *et al*: CircRNA LRP6 promotes the development of osteosarcoma via negatively regulating KLF2 and APC levels. Am J Transl Res 11: 4126-4138, 2019.
15. Zhang Q, Jiang C, Ren W, Li S, Zheng J, Gao Y, Zhi K and Gao L: Circ-LRP6 mediates epithelial-mesenchymal transition and autophagy in oral squamous cell carcinomas. J Oral Pathol Med 50: 660-667, 2021.
16. Wang J, Zhu W, Tao G and Wang W: Circular RNA circ-LRP6 facilitates Myc-driven tumorigenesis in esophageal squamous cell cancer. Bioengineered 11: 932-938, 2020.
17. Yu Y, Wang L, Li Z, Zheng Y, Shi Z and Wang G: Long noncoding RNA CRNDE functions as a diagnostic and prognostic biomarker in osteosarcoma, as well as promotes its progression via inhibition of miR-335-3p. J Biochem Mol Toxicol 35: e22734, 2021.
18. Gulino R, Forte S, Parenti R, Memeo L and Gulisano M: MicroRNA and pediatric tumors: Future perspectives. Acta Histochem 117: 339-354, 2015.
19. Liu Y, Wang Y, Yang H, Zhao L, Song R, Tan H and Wang L: MicroRNA-873 targets HOXA9 to inhibit the aggressive phenotype of osteosarcoma by deactivating the Wnt/β-catenin pathway. Int J Oncol 54: 1809-1820, 2019.
20. Gao S, Wang J, Tian S and Luo J: miR-9 depletion suppresses the proliferation of osteosarcoma cells by targeting p16. Int J Oncol 54: 1921-1932, 2019.
21. Feng T, Zhu Z, Jin Y, Wang H, Mao X, Liu D, Li Y, Lu L and Zuo G: The microRNA-708-5p/ZEB1/EMT axis mediates the metastatic potential of osteosarcoma. Oncol Rep 43: 491-502, 2020.
22. Sun X, Xu Y, Zhang S, Li X, Wang Y, Zhang Y, Zhao X, Li Y and Wang Y: MicroRNA-183 suppresses the vitality, invasion and migration of human osteosarcoma cells by targeting metastasis-associated protein 1. Exp Ther Med 15: 5058-5064, 2018.
23. Zhao X, Xu Y, Sun X, Ma Y, Zhang Y, Wang Y, Guan H, Jia Z, Li Y and Wang Y: miR-17-5p promotes proliferation and epithelial-mesenchymal transition in human osteosarcoma cells by targeting SRC kinase signaling inhibitor 1. J Cell Biochem 120: 5495-5504, 2019.
24. Wang N, Li P, Liu W, Wang N, Lu Z, Feng J, Zeng X, Yang J, Wang Y and Zhao W: miR-141-3p suppresses proliferation and promotes apoptosis by targeting GLI2 in osteosarcoma cells. Oncol Rep 39: 747-754, 2018.
25. Wang L: MiR-141-3p overexpression suppresses the malignancy of osteosarcoma by targeting FUS to degrade LDHB. Biosci Rep: Jun 26, 2020 (Epub ahead of print).
26. Liang Z, Li X, Liu S, Li C, Wang X and Xing J: MiR-141-3p inhibits cell proliferation, migration and invasion by targeting TRAF5 in colorectal cancer. Biochem Biophys Res Commun 514: 699-705, 2019.
27. Zhou Y, Zhong JH, Gong FS and Xiao J: MiR-141-3p suppresses gastric cancer induced transition of normal fibroblast and BMSC to cancer-associated fibroblasts via targeting STAT4. Exp Mol Pathol 107: 85-94, 2019.
28. Jiang J, Sun Y, Xu G, Wang H and Wang L: The role of miRNA, lncRNA and circRNA in the development of intervertebral disk degeneration (review). Exp Ther Med 21: 555, 2021.

29. Chen F, He L, Qiu L, Zhou Y, Li Z, Chen G, Xin F, Dong X, Xu H, Wang G, *et al*: Circular RNA CircEPB41L2 functions as tumor suppressor in hepatocellular carcinoma through sponging miR-590-5p. Cancer Manag Res 13: 2969-2981, 2021.
30. Zhang C, Cao J, Lv W and Mou H: CircRNA_100395 carried by exosomes from adipose-derived mesenchymal stem cells inhibits the malignant transformation of non-small cell lung carcinoma through the miR-141-3p-LATS2 axis. Front Cell Dev Biol 9: 663147, 2021.
31. Huang XY, Huang ZL, Zhang PB, Huang XY, Huang J, Wang HC, Xu B, Zhou J and Tang ZY: CircRNA-100338 is associated with mTOR signaling pathway and poor prognosis in hepatocellular carcinoma. Front Oncol 9: 392, 2019.
32. Chao F, Song Z, Wang S, Ma Z, Zhuo Z, Meng T, Xu G and Chen G: Novel circular RNA circSOBP governs amoeboid migration through the regulation of the miR-141-3p/MYPT1/p-MLC2 axis in prostate cancer. Clin Transl Med 11: e360, 2021.
33. Ma J, Wu Y and He Y: Silencing circRNA LRP6 down-regulates PRMT1 to improve the streptozocin-induced pancreatic β-cell injury and insulin secretion by sponging miR-9-5p. J Bioenerg Biomembr 53: 333-342, 2021.
34. Xue J, Chen C, Luo F, Pan X, Xu H, Yang P, Sun Q, Liu X, Lu L, Yang Q, *et al*: CircLRP6 regulation of ZEB1 via miR-455 is involved in the epithelial-mesenchymal transition during arsenite-induced malignant transformation of human keratinocytes. Toxicol Sci 162: 450-461, 2018.
35. Cai JY, Xu TT, Wang Y, Chang JJ, Li J, Chen XY, Chen X, Yin YF and Ni XJ: Histone deacetylase HDAC4 promotes the proliferation and invasion of glioma cells. Int J Oncol 53: 2758-2768, 2018.
36. Xiao Q, Huang L, Zhang Z, Chen X, Luo J, Zhang Z, Chen S, Shu Y, Han Z and Cao K: Overexpression of miR-140 inhibits proliferation of osteosarcoma cells via suppression of histone deacetylase 4. Oncol Res 25: 267-275, 2017.
37. Zeng LS, Yang XZ, Wen YF, Mail SJ, Wang MH, Zhang MY, Zheng XF and Wang HY: Overexpressed HDAC4 is associated with poor survival and promotes tumor progression in esophageal carcinoma. Aging (Albany NY) 8: 1236-1249, 2016.
38. Cao K, Wang H, Fang Y, Wang Y, Wei L, Chen X, Jiang Z, Wei X and Hu Y: Histone deacetylase 4 promotes osteosarcoma cell proliferation and invasion by regulating expression of proliferating cell nuclear antigen. Front Oncol 9: 870, 2019.
39. Wang H, Feng L, Zheng Y, Li W, Liu L, Xie S, Zhou Y, Chen C and Cheng D: LINC00680 promotes the progression of non-small cell lung cancer and functions as a sponge of miR-410-3p to enhance HMGB1 expression. Onco Targets Ther 13: 8183-8196, 2020.
40. Zhang H, Wang J, Li J, Zhou X, Yin L, Wang Y, Gu Y, Niu X, Yang Y, Ji H and Zhang Q: HMGB1 is a key factor for tamoxifen resistance and has the potential to predict the efficacy of CDK4/6 inhibitors in breast cancer. Cancer Sci 112: 1603-1613, 2021.
41. Nakamura T, Okui T, Hasegawa K, Ryumon S, Ibaragi S, Ono K, Kunisada Y, Obata K, Masui M, Shimo T and Sasaki A: High mobility group box 1 induces bone pain associated with bone invasion in a mouse model of advanced head and neck cancer. Oncol Rep 44: 2547-2558, 2020.
42. Zhu X, Sun L and Wang Y: High mobility group box 1 (HMGB1) is upregulated by the Epstein-Barr virus infection and promotes the proliferation of human nasopharyngeal carcinoma cells. Acta Otolaryngol 136: 87-94, 2016.
43. Yuan C and Yang L: Long non-coding RNA PITPNA-AS1 accelerates the progression of colorectal cancer through miR-129-5p/HMGB1 axis. Cancer Manag Res 12: 12497-12507, 2020.
44. Guan H, Liu J, Lv P, Zhou L, Zhang J and Cao W: MicroRNA-590 inhibits migration, invasion and epithelial-to-mesenchymal transition of esophageal squamous cell carcinoma by targeting low-density lipoprotein receptor-related protein 6. Oncol Rep 44: 1385-1392, 2020.
45. Zhang F, Cheng N, Du J, Zhang H and Zhang C: MicroRNA-200b-3p promotes endothelial cell apoptosis by targeting HDAC4 in atherosclerosis. BMC Cardiovasc Disord 21: 172, 2021.
46. Lu Z, Wang D, Wang X, Zou J, Sun J and Bi Z: MiR-206 regulates the progression of osteoporosis via targeting HDAC4. Eur J Med Res 26: 8, 2021.
47. Gondaliya P, P Dasare A, Jash K, Tekade RK, Srivastava A and Kalia K: miR-29b attenuates histone deacetylase-4 mediated podocyte dysfunction and renal fibrosis in diabetic nephropathy. J Diabetes Metab Disord 19: 13-27, 2019.
48. Malavika D, Shreya S, Raj Priya V, Rohini M, He Z, Partridge NC and Selvamurugan N: miR-873-3p targets HDAC4 to stimulate matrix metalloproteinase-13 expression upon parathyroid hormone exposure in rat osteoblasts. J Cell Physiol 235: 7996-8009, 2020.
49. Zhang Y, Chu X and Wei Q: MiR-451 Promotes cell apoptosis and inhibits autophagy in pediatric acute myeloid leukemia by targeting HMGB1. J Environ Pathol Toxicol Oncol 40: 45-53, 2021.
50. Feng XE: miR-548b suppresses melanoma cell growth, migration, and invasion by negatively regulating its target gene HMGB1. Cancer Biother Radiopharm 36: 189-201, 2021.
51. Shen H, Xu L, You C, Tang H, Wu H, Zhang Y and Xie M: miR-665 is downregulated in glioma and inhibits tumor cell proliferation, migration and invasion by targeting high mobility group box 1. Oncol Lett 21: 156, 2021.
52. Dong H and Song J: miR-142-3p reduces the viability of human cervical cancer cells by negatively regulating the cytoplasmic localization of HMGB1. Exp Ther Med 21: 212, 2021.
53. Qiu M, Liu D and Fu Q: MiR-129-5p shuttled by human synovial mesenchymal stem cell-derived exosomes relieves IL-1β induced osteoarthritis via targeting HMGB1. Life Sci 269: 118987, 2021.
54. Livak KJ and Schmittgen TD: Analysis of relative gene expression data using real-time quantitative PCR and the 2(-Delta Delta C(T)) method. Methods 25: 402-408, 2001.
55. Liu W, Zhang J, Zou C, Xie X, Wang Y, Wang B, Zhao Z, Tu J, Wang X, Li H, *et al*: Microarray expression profile and functional analysis of circular RNAs in osteosarcoma. Cell Physiol Biochem 43: 969-985, 2017.
56. Guan H, Mei Y, Mi Y, Li C, Sun X, Zhao X, Liu J, Cao W, Li Y and Wang Y: Downregulation of lncRNA ANRIL suppresses growth and metastasis in human osteosarcoma cells. Onco Targets Ther 11: 4893-4899, 2018.
57. Lei S and Xiang L: Up-regulation of circRNA hsa_circ_0003074 expression is a reliable diagnostic and prognostic biomarker in patients with osteosarcoma. Cancer Manag Res 12: 9315-9325, 2020.
58. Nie WB, Zhao LM, Guo R, Wang MX and Ye FG: Circular RNA circ-NT5C2 acts as a potential novel biomarker for prognosis of osteosarcoma. Eur Rev Med Pharmacol Sci 22: 6239-6244, 2018.
59. Kun-Peng Z, Chun-Lin Z, Jian-Ping H and Lei Z: A novel circulating hsa_circ_0081001 act as a potential biomarker for diagnosis and prognosis of osteosarcoma. Int J Biol Sci 14: 1513-1520, 2018.
60. Wang Z, Deng M, Chen L, Wang W, Liu G, Liu D, Han Z and Zhou Y: Circular RNA Circ-03955 promotes epithelial-mesenchymal transition in osteosarcoma by regulating miR-3662/metadherin pathway. Front Oncol 10: 545460, 2020.
61. Wan J, Liu Y, Long F, Tian J and Zhang C: circPVT1 promotes osteosarcoma glycolysis and metastasis by sponging miR-423-5p to activate Wnt5a/Ror2 signaling. Cancer Sci 112: 1707-1722, 2021.
62. Yi Y, Liu Y, Wu W, Wu K and Zhang W: Reconstruction and analysis of circRNA-miRNA-mRNA network in the pathology of cervical cancer. Oncol Rep 41: 2209-2225, 2019.
63. Zhang J, Yang Y, Yang T, Liu Y, Li A, Fu S, Wu M, Pan Z and Zhou W: microRNA-22, downregulated in hepatocellular carcinoma and correlated with prognosis, suppresses cell proliferation and tumourigenicity. Br J Cancer 103: 1215-1220, 2010.
64. Hsieh TH, Hsu CY, Tsai CF, Long CY, Chai CY, Hou MF, Lee JN, Wu DC, Wang SC and Tsai EM: miR-125a-5p is a prognostic biomarker that targets HDAC4 to suppress breast tumorigenesis. Oncotarget 6: 494-509, 2015.
65. Shen YF, Wei AM, Kou Q, Zhu QY and Zhang L: Histone deacetylase 4 increases progressive epithelial ovarian cancer cells via repression of p21 on fibrillar collagen matrices. Oncol Rep 35: 948-954, 2016.
66. Zhang Y, Lv F, Qiao L and Zhao Q: MiR-505 inhibits prostate cancer cell invasion, metastasis and epithelial-to-mesenchymal transition through targeting HMGB-1. J BUON 25: 2036-2044, 2020.
67. Luan X, Ma C, Wang P and Lou F: HMGB1 is negatively correlated with the development of endometrial carcinoma and prevents cancer cell invasion and metastasis by inhibiting the process of epithelial-to-mesenchymal transition. Onco Targets Ther 10: 1389-1402, 2017.
68. Meng Q, Zhao J, Liu H, Zhou G, Zhang W, Xu X and Zheng M: HMGB1 promotes cellular proliferation and invasion, suppresses cellular apoptosis in osteosarcoma. Tumour Biol 35: 12265-12274, 2014.